ACS Sustainable Chemistry & Engineering

Research Article

pubs.acs.org/journal/ascecg

Superior Performance of Fully Biobased Poly(lactide) via Stereocomplexation-Induced Phase Separation: Structure versus Property

Piming Ma,*[,†,‡] Tianfeng Shen,[†] Pengwu Xu,[†] Weifu Dong,[†] Piet J. Lemstra,[‡] and Mingqing Chen*[,†]

[†]The Key Laboratory of Food Colloids and Biotechnology, Ministry of Education, School of Chemical and Material Engineering, Jiangnan University, 1800 Lihu Road, Wuxi 214122, China

[‡]Department of Chemical Engineering and Chemistry, Eindhoven University of Technology, Eindhoven 5612 AZ, The Netherlands

ABSTRACT: Superior properties such as high strength, toughness and transparency of fully biobased poly(lactide) (PLA) were achieved simultaneously without any external modifiers. The improvement in properties is well explained by a structural/morphological study. Stereocomplex PLA (SC-PLA) was obtained by melt compounding asymmetric poly(L-lactide)/poly(D-lactide) (PLLA/PDLA) blends at 200 °C and confirmed by wide-angle X-ray diffraction (WAXD) and differential scanning calorimetry (DSC) analyses. The SC-PLA domains (d = 950−1200 nm) lead to a physical cross-link network in the PLLA matrix. Rheology and Molau experiment reveal two different microstructures as a function of SC-PLA content, i.e., the connection of SC-PLA domains varied from chain entanglement to direct molecular bridging when the SC-PLA content increased from 10% to 23%. The SC-PLA crystals and the cross-link network reinforced the PLLA matrix, resulting in increases in melt viscosity, modulus and yield strength. Surprisingly, the elongation at break of the PLLA/PDLA blends was increased concomitantly from 11% to 200% with the SC-PLA content up to 10%. The brittle-to-ductile transition is ascribed to the cross-link network and easy deformation/cavitation of the SC-PLA domains. In addition, the asymmetric PLLA/PDLA blends exhibit an average visible light transmittance as high as 70% and the blends showed excellent heat-resistance after a short annealing at 100 °C.

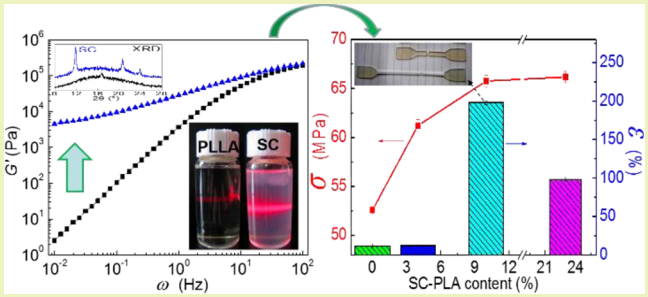

KEYWORDS: *Poly(lactide), Stereocomplexation, Microstructure, Properties*

INTRODUCTION

Biobased and biodegradable polymeric materials such as poly(lactide) (PLA) have received considerable attention in the past decades due to the environmental concern and sustainability issues associated with petroleum-based polymers.[1,2] Several favorable properties like strength, stiffness and transparency at room temperature make PLA promising as a substitute for traditional plastics. However, it is challenging to achieve high technical applications due to PLA's brittleness and low heat distortion temperature associated with a T_g around 55 °C and low crystallinity.[3−6]

Many efforts have been made to improve the toughness of PLA such as plasticization,[6,7] copolymerization[8,9] and compounding with other materials.[10−25] Flexible (co)polymers including poly(hydroxyalkanoate)s,[10] poly(β-caprolactone),[12,13] poly(butylene succinate),[14,15] poly(butylene adipate-*co*-terephthalate),[16] poly(butylene succinateco-adipate),[17] POSS−rubber−PDLA nanoparticles,[18] poly(urethane),[19] ethylene−vinyl acetate rubber,[20] ethylene−glycidyl methacrylate copolymer,[21] plant oil,[22] ethylene−acrylate copolymer,[23] ethylene−octene copolymer[24] and natural rubber[25] were used to modify PLA. Tough(er) PLA-based materials were obtained via the above techniques, which, however, resulted in low(er) stiffness and strength. Moreover, biobased and/or biodegradable features of the PLA were compromised when blending with conventional (co)polymers. On the other hand, PLA was also reinforced by inorganic fillers accompanied by deterioration in toughness and transparency.[28−30] Therefore, it is of interest to prepare fully biobased and biodegradable PLA materials with superior and balanced performance.

Poly(L-lactide) (PLLA) and its enantiomeric opposite, viz. poly(D-lactide) (PDLA), can form a stereocomplex (SC) upon mixing. SC-PLA possesses superior physicomechanical properties such as a melting point of 220−230 °C, which is 50 °C higher than that of the PLA homopolymer.[31−33] Although much attention has been paid to stereocomplexation of symmetric PLLA/PDLA (50/50) blends,[34,35] it is still challenging in practice to achieve high SC content because of a kinetic reason and degradation of PLA chains at a temperature higher than the melting point of SC-PLA.[35] As a consequence, solution mixing was preferably used in fundamental research.

Received: March 15, 2015
Revised: May 26, 2015
Published: May 27, 2015

DOI: 10.1021/acssuschemeng.5b00208
ACS Sustainable Chem. Eng. 2015, 3, 1470−1478

Recently, high volume SC-PLA (crystallization enthalpy $\Delta H_{c\text{-}sc}$ = 34 J/g_{PLA}) was obtained in symmetric PLLA/PDLA blends by incorporation of poly(methyl methacrylate) (PMMA)[36] or poly(ethylene glycol) (PEG).[37] Good processability, heat-resistance and optical clarity of the PLLA/PDLA/PMMA ternary blends were achieved without a discussion in mechanical behavior.[36] A SC crystallite network was detected in asymmetric PLLA/PDLA blends with 2−5 wt % of PDLA,[38] and the SC-PLA speeded up the crystallization of the PLLA matrix.[38−40] However, the effect of the SC crystallite network on properties of the asymmetric PLLA/PDLA blends is not yet clear. In another study, PLLA/PDLA (50/50) films showed higher tensile strength and modulus than neat PLLA films ascribing to a stereocomplexation-induced cross-link network, but the elongation at break of the PLLA/PDLA(50/50) films was even lower than 10%.[41]

The prime objective of this work is to prepare complete PLA materials via melt compounding, viz. asymmetric PLLA/PDLA blends with superior and balanced properties. The stereocomplexation, microstructures, mechanical properties, toughening mechanism, light transmittance and heat-resistance of the materials were systematically investigated.

The authors hasten to remark that the developed materials in this work are fully originated from renewable resources, and they are biodegradable and compostable after disposal without any harmful residuals. From an energy and environment point of view, these materials show obvious sustainability and can be a substitute for parts of traditional petroleum-based plastics considering their superior properties. Moreover, the developed materials are easily processable and recyclable as well. Therefore, this work has beyond pure academic interest.

EXPERIMENTAL SECTION

Materials. Poly(L-lactide) (PLLA, 4032D) was purchased from Nature Works LLC, USA, with a M_n = 135 kDa and PDI = 1.7. The content of L-lactide in the PLLA is approximately 98%. Poly(D-lactide) (PDLA, experimental grade) with a M_n = 86 kDa and PDI = 1.8 was provided by PURAC, The Netherlands. The content of D-lactide in the PDLA is approximately 99%.

Sample Preparation. PLLA and PDLA were dried at 70 °C in a vacuum oven for 12 h before use. All the samples were prepared in a mixing chamber of a rheometer (RM-200, HABO Electrical Appliance Manufacturing Company, China) at 200 °C and 30 rpm for 5 min. The weight ratio of PLLA/PDLA blends was designed between 100/0 and 80/20. The samples were then compressed into sheets at 200 °C and 15 MPa for 2 min using a hot compression molding machine and subsequently cooled down with room-temperature compression plates at a pressure of 5 MPa. The compression-molded samples were used for characterization.

Characterization. *Differential Scanning Calorimetry (DSC).* The crystallization and melting behavior of the PLLA/PDLA blends were investigated by using DSC (204F1, NETZSCH Gerätebau GmbH, Germany). The samples were heated in a nitrogen atmosphere from 0 to 250 °C at a heating rate of 10 °C/min. To correlate the properties and SC-PLA content, the first DSC heating curves were recorded. The crystallinity of HC-PLA (X_{hc}) is calculated via $X_{hc} = (H_{m\text{-}hc} - H_{cc})/H_m^0 \times 100\%$,[42] where $H_{m\text{-}hc}$ and H_{cc} are melt enthalpy and cold crystallization enthalpy of the HC-PLA; the crystallinity of SC-PLA (X_{sc}) is calculated via $X_{sc} = H_{m\text{-}sc}/H_m^0 \times 100\%$, where $H_{m\text{-}sc}$ is the melt enthalpy of SC-PLA. The H_m^0 is the fusion enthalpy of 100% HC-PLA and SC-PLA, i.e., 93.3 and 142 J/g, respectively.[42]

Wide Angle X-ray diffraction (WAXD). WAXD measurements were carried out using an X-ray diffractometer (Bruker AXS D8, Germany) equipped with a Ni-filtered Cu Kα radiation source with a wavelength of 1.542 Å. The measurements were operated at 40 kV and 40 mA with scan angles from 5° to 35° and a scan rate of 3°/min.

Rheological Behavior. Dynamic rheological experiments were carried out on a DHR-2 rheometer (TA Instruments, USA) in a plate−plate configuration (25 mm in diameter and 1 mm in gap) at 200 °C. The samples were examined in a frequency-sweep mode, from 100 to 0.01 Hz, with a constant strain of 1%. The strain was predetermined from a strain-sweep experiment to ensure the test was performed in the linear viscoelastic range.

Molau Experiment. A Molau experiment was done by dipping PLLA, PDLA and PLLA/PDLA blends in chloroform (~30 mg/mL). The mixtures were sealed in glass bottles for 3 days and then digital photos were taken. The Tyndall effect was checked by using a red laser light through the bottles when the photos were taken.

Dynamic Light Scattering (DLS). DLS measurements were carried out using a Zeta PALS ζ-potential and particle analyzer (Brookhaven Instruments Corporation, USA) to analyze the particle sizes of SC-PLA in the PLLA/PDLA suspensions. The suspensions for light scattering were prepared with chloroform (~0.1 mg/mL).

Mechanical Properties. Tensile properties of the PLLA/PDLA samples were tested using a universal tester (Instron 5967, USA) according to GBT529-2008 at a crosshead speed of 10 mm/min. The geometry of the parallel section of the tensile bar is 25 × 4 × 1 mm. Five specimens of each sample were examined and the averaged values were presented. All the tests were performed at room temperature.

Transmission Electron Microscopy (TEM). TEM was performed using a JEM-2100 microscope, operated at 200 kV. Ultrathin sections (80 nm) were obtained at −60 °C using a Leica Ultracut microtome. The ultrathin sections from different parts of the tensile bar were subjected to TEM characterization without staining.

Visible Light Transmittance. The transparency of the PLLA/PDLA films (1.0 mm in thickness) was investigated using an UV−visible spectrophotometer (TU-1901, Beijing Purkinje General Instrument Co. Ltd.). The air was used as blank reference, and transmittance spectra were recorded in the wavelength range from 400 to 800 nm.

Dynamic Mechanical Analysis (DMA). DMA-Q800 (TA Instruments) was performed to measure the dynamic mechanical properties and thermal behavior of the asymmetric PLLA/PDLA blends. The specimens (15 × 5.3 × 1.0 mm) were heated in a tensile-film mode from room temperature to 130 °C at 3 °C/min. The amplitude and frequency were set as 20 μm and 1 Hz, respectively. The storage modulus and loss modulus were recorded.

RESULTS AND DISCUSSION

Stereocomplexation in the PLLA Matrix. SC-PLA was created by melt compounding PLLA with 2.5−20 wt % of PDLA at 200 °C in this work. SC-PLA can be distinguished easily from homocrystal PLA (HC-PLA) by WAXD. The 1D-WAXD patterns of the PLLA/PDLA blends as a function of PDLA content are shown in Figure 1. A broad diffraction peak is observed for both of PLLA and PDLA showing an amorphous feature of the neat materials. After addition of 2.5

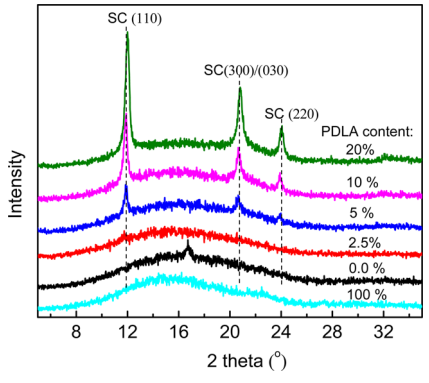

Figure 1. 1D-WAXD patterns of PLLA/PDLA blends with different amounts of PDLA showing the formation of SC-PLA.

DOI: 10.1021/acssuschemeng.5b00208
ACS Sustainable Chem. Eng. 2015, 3, 1470−1478

wt % of PDLA into PLLA, an indistinctive but still visible peak at $2\theta = 11.8°$ is detected, which is assigned to the [110] plane of SC-PLA. Meanwhile, another two peaks located at $2\theta = 20.8$ and 23.8° are observed at 5 wt % of PDLA corresponding to the [300/030] and [220] planes of the SC-PLA, respectively.[43] The intensity of the peaks was enhanced with increasing the PDLA content. On the other hand, diffraction peaks ($2\theta = 16°$, 18.4° and 21.8°) of HC-PLLA and diffraction peaks ($2\theta = 16.6°$ and 18.9°) of HC-PDLA are absent in the studied formulations. These results confirm that (i) different amounts of SC-PLA are obtained in the asymmetric PLLA/PDLA blends and (ii) the concentration of HC-PLA is too low to be detected.

The stereocomplexation behavior of the asymmetric PLLA/PDLA blends was further studied by using DSC. Figure 2a shows the first heating DSC curves of the PLLA, PDLA and PLLA/PDLA blends. Four transitions were identified, i.e., glass transition of PLA (T_g), cold crystallization of PLA (T_{cc}), melting of HC-PLA ($T_{m\text{-}hc}$) and melting of SC-PLA ($T_{m\text{-}sc}$), respectively. A $T_{m\text{-}sc}$ at 219 °C is visible for the blend with 5 wt % of PDLA, and this peak become stronger and increased to 227 °C with the PDLA content up to 20 wt %. It indicates that higher thickness and/or more perfection of SC lamellae was achieved when the PLLA/PDLA blends approached to symmetric system. In contrast, a decrease in $T_{m\text{-}hc}$ of the PLLA from 172 to 167 °C was obtained. This phenomenon is different from a previous report[38] where no influence of SC-PLA on the $T_{m\text{-}hc}$ was observed. The crystallinity of the HC-PLA (X_{hc}) and SC-PLA (X_{sc}) are presented in Figure 2b. Apparently, the X_{sc} is linearly proportional to the PDLA content in the range of 5−20 wt %, below which the SC-PLA is not detectable by DSC. According to these data, the efficiency of stereocomplexation (E_{sc}) is determined as 42−57%, as presented in the inset of Figure 2b. Following a different trend, the HC-PLA is in a low and constant concentration (≤3%) as a function of PDLA content. It has to be noted that the calculation of X_{hc} and X_{sc} is based on melt enthalpy from DSC data, which may be influenced by cold crystallization and recrystallization of HC and SC crystals upon heating. The content of SC in the cold crystallization enthalpy is expected to be very low because the temperature range of 90−110 °C is unfavorable for PLA stereocomplexation but favorable for the cold crystallization of HC-PLA.[10,37]

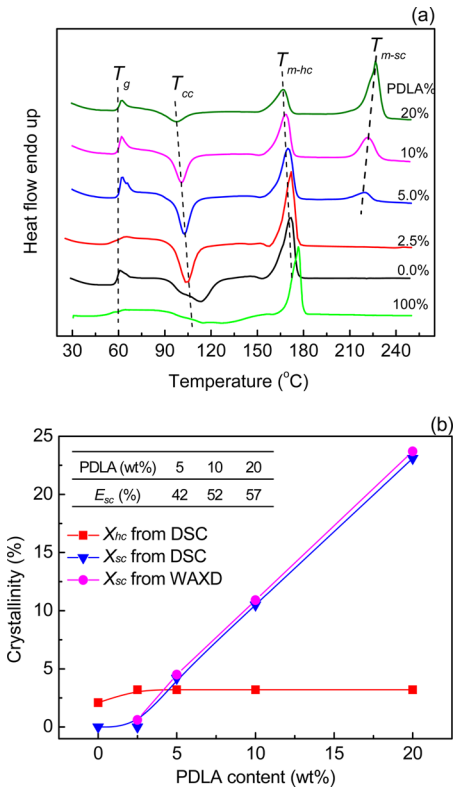

Figure 2. (a) First heating DSC curves (10 °C/min) of the asymmetric PLLA/PDLA blends with different PDLA contents and (b) corresponding crystallinity of the SC-PLA (X_{sc}) and HC-PLA (X_{hc}). The efficiency of stereocomplexation (E_{sc}) is inset into panel b.

Consequently, seldom HC crystals in the PLLA/PDLA blends were detected by WAXD (Figure 1); meanwhile, the melt enthalpy of HC-PLA ($H_{m\text{-}hc}$) from DSC measurement is comparable to the corresponding cold crystallization enthalpy (H_{cc}). These results evidenced that the X_{sc} should be dominantly from the previous melt compounding process rather than from the cold crystallization. On the other hand, recrystallization usually leads to multimelting behavior upon heating (melt/recrystallization/remelt mechanism).[44] In this work, neither HC nor SC crystals showed multimelting peaks, indicating that the recrystallization was not so significant. Therefore, the X_{hc} and X_{sc} values reported here are valuable for discussion, although the cold crystallization and recrystallization of SC cannot be fully excluded by the DSC results.

WAXD patterns were recorded at room temperature, which is free of cold crystallization and recrystallization. The X_{sc} values from WAXD patterns are plotted in Figure 2b for comparison. Apparently, the X_{sc} values obtained from the WAXD measurements are consistent with that from the DSC results, which well supports the above arguments.

Effect of Stereocomplexation on the Rheology and Structure of the Asymmetric PLLA/PDLA Blends. Viscoelastic response of the asymmetric PLLA/PDLA blends was investigated by oscillatory shear rheological measurements at 200 °C. At such a temperature, the PLLA matrix ($T_m \sim 165$ °C) is in a molten state whereas the SC-PLA ($T_m \sim 220$ °C) is still in the rigid crystalline form. The storage modulus (G'), complex viscosity (η^*), loss modulus (G'') and loss tangent ($\tan\delta$) of the blends as a function of frequency and SC-PLA content are shown in Figure 3.

For linear polymer, e.g., PLLA in Figure 3a,b, the slopes of $\log(G')$ versus $\log(\omega)$ and $\log(G'')$ versus $\log(\omega)$ roughly follow the terminal scaling law, i.e., $G' \propto \omega^2$ and $G'' \propto \omega^1$ at the low frequency region. On the other hand, the $\log(G')$ versus $\log(\omega)$ of the PLLA/PDLA blends shows pronounced deviation from slope 2, and the G' of the blends increases with the SC-PLA content. The PLLA/PDLA blends with SC-PLA content higher than 4% exhibit a notable solid-like behavior at the low frequency zone (Figure 3a). These phenomena indicate a slower relaxation process and an increased elasticity of the PLLA/PDLA melt due to the existence of SC-PLA.[45] Similar trends are observed for $\log(G'')$ versus $\log(\omega)$, as shown in Figure 3b.

In Figure 3c, neat PLLA shows a Newtonian plateau at the low frequency zone, whereas a non-Newtonian behavior in the presence of SC-PLA is observed, i.e., the slopes of $\log(\eta^*)$ versus $\log(\omega)$ deviate from 0 to −1. Apparently, branched and/or cross-link structures exist in the PLLA/PDLA blends. It has to be remarked that the melts retain good processability even at a SC-PLA concentration of 10%.

DOI: 10.1021/acssuschemeng.5b00208
ACS Sustainable Chem. Eng. 2015, 3, 1470−1478

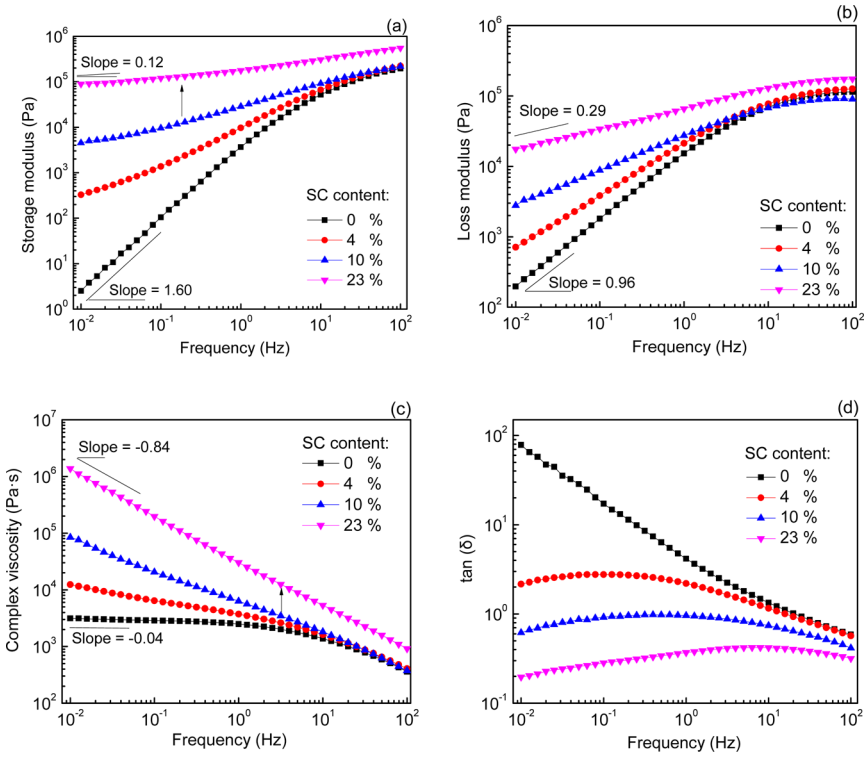

Figure 3. (a) Storage modulus (G'), (b) loss modulus (G''), (c) complex viscosity (η^*) and (d) tan δ of the asymmetric PLLA/PDLA melts at 200 °C as a function of SC-PLA content and frequency.

The ratio of G'' to G', viz. tan δ, was used to study the microstructure of the asymmetric PLLA/PDLA blends due to its sensitivity to relaxation.[46] The tan δ of PLLA decreases monotonically with increasing the frequency (Figure 3d), which is a typical rheological behavior of a viscoelastic liquid. The tan δ decreased dramatically with increasing the SC-PLA concentration; meanwhile, broad tan δ peaks were observed. These results demonstrate an enhanced elastic response and a network in the PLLA/PDLA melts. Similarly, a critical network was also observed above 2.0 wt % of PDLA in a previous study.[38]

A suspension-like structure is expected in the asymmetric PLLA/PDLA melts because SC-PLA cannot be dissolved in the PLLA matrix at 200 °C. Consequently, the suspended SC-PLA has roles of both rigid filler and physical cross-link points. The reinforcing effect of the "rigid filler" is evidenced by an increase in G' and η^*, whereas the cross-link network is confirmed by a nearly frequency-independence of G' and tan δ at a low frequency zone. It is noticed that the G', G'' and η^* of the blends with 23% of SC-PLA are far higher than the other examined blends. It is related to the higher SC-PLA content whereas may also be due to different cross-link structures. Therefore, the enhancement in the G', G'' and η^* are resulted from both of the increase in SC crystallinity and the cross-link structures.

A cross-link network is important to rheology, mechanical and processing properties of a polymeric material. Horst and Coppola et al. reported a critical gel point in a semicrystalline polymer system with crystallinity as low as 1.0−1.5%.[47,48] At low crystallinity, the adjacent crystalline domains are connected by amorphous molecules, i.e., molecules that embedded only in one of the SC domains (coded as Structure I).[38,47] Molau experiments were carried out to monitor the cross-link structures using chloroform as a solvent, as shown in Figure 4. Chloroform is a good solvent for PLLA but not for SC-PLA. A transparent solution was obtained for neat PLLA (Figure 4A), whereas stable suspensions were observed for the PLLA/PDLA blends at SC-PLA concentrations lower than 10% (Figure 4B,C). These results are consistent with a previous study referring to Structure I.[38] However, both suspension and large pieces of gel were observed at 23% of SC-PLA (Figure 4D). Because no chemical reaction was expected in blending PLLA with PDLA, the gel confirms another kind of cross-link structure, viz. the adjacent crystalline domains are connected by molecules with segments participated in both of the adjacent crystalline domains (coded as Structure II). The SC-PLA domain size in the suspensions was further analyzed by

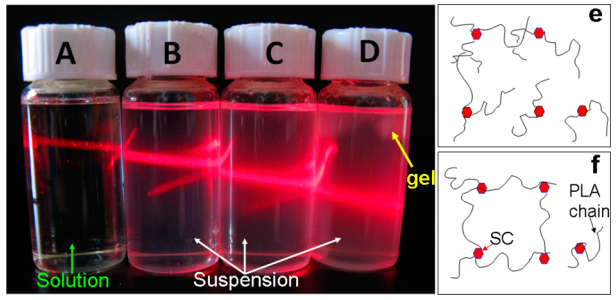

Figure 4. Digital photos of the asymmetric PLLA/PDLA blends in chloroform with SC-PLA concentrations (A) 0%, (B) 4%, (C) 10% and (D) 23%, and schematic illustration of the cross-link structures: (e) Structure I referring to low SC concentration and (f) Structure II referring to high SC concentration. The Tyndall effect was carried out by using a red laser light through the bottles. The SC-PLA domain size in suspensions A, B and C is 950 ± 45, 1075 ± 15 and 1215 ± 80 respectively, measured via DLS. The photo was taken 72 h after dissolving.

DOI: 10.1021/acssuschemeng.5b00208
ACS Sustainable Chem. Eng. 2015, 3, 1470−1478

dynamic light scattering (DLS). A size of 950−1200 nm was obtained with increasing the SC-PLA content from 4% to 23%. It has to be addressed that a mixture of PLLA and PDLA (80/20, without melt compounding) in chloroform showed the same phenomenon as that shown in Figure 4A, i.e., clear solution without a noticeable Tyndall effect (not shown). This phenomenon rules out the interference of possible stereocomplexation in the dissolution process on the argument.

It can be concluded from the Molau experiments that Structure I is dominant at low SC-PLA concentrations (<10%), whereas Structure II plays the decisive role at SC-PLA concentrations higher than 23%. Structures I and II are schematically illustrated in Figure 4e,f, respectively. The two kinds of structures may coexist in the asymmetric PLLA/PDLA systems, depending on the concentration of the SC-PLA domains.

Mechanical Properties of the PLLA/PDLA Blends. The mechanical properties of the PLLA/PDLA blends as a function of SC-PLA concentration were studied via uniaxial tensile test. The results are abbreviated in Figure 5. The yield strength of

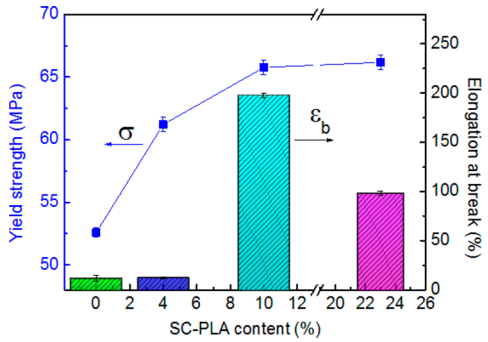

Figure 5. Yield stress (σ) and elongation at break (ε_b) of the PLLA/PDLA blends as a function of SC-PLA content.

PLLA was increased from 52.5 to 66.5 MPa with the SC-PLA concentration up to 10% and then leveled off. In the literature, the tensile strength of PLLA was also enhanced via stereocomplexation but low in elongation at break (typically ε_b < 5%).[41,49−51] Surprisingly, a ε_b of 200% of a PLLA/PDLA blend with 10 wt % of PDLA was achieved, which is 20 times higher than that of neat PLLA. These results display both the reinforcing and toughening effects of SC-PLA on the PLLA matrix. Liu and his co-workers recently reported that PLLA could be toughened by 30 wt % of PDLA-*b*-PEG-*b*-PDLA (solution mixing), leading to a ε_b up to 130%.[52] The improvement in toughness was ascribed to a synergistic effect of stereocomplexation and plasticization from PEG segments. Apparently, the "synergistic effect" could not adapt to the present PLLA/PDLA system because no plasticizers such as PEG exist here.

Tsuji et al. reported tensile properties of PLLA/PDLA (PDLA < 10 wt %) blends with ε_b < 9% and tensile strength <55 MPa, which were lower than the present results. This might result from differences in sample preparation method, molecular weight of PLA, tensile bar geometry and tensile speed. More important, the PLLA/PDLA samples in the literature[51] were annealed at 135 °C for 10 h, leading to a crystallinity of PLLA matrix as high as 63% before subjected to tensile test. It thus reasonably resulted in brittleness.

The reinforcing and toughening effect of the SC-PLA on the PLLA matrix is then explained by the stereocomplexation-induced phase separation, which led to different SC crystallinities and physical networks in the asymmetric PLLA/PDLA blends and the deformation/cavitation of SC-PLA domains upon stretching. The physical network was already proven by rheological/Molau analysis, and the proposed deformation/cavitation mechanism will be discussed below. The amorphous feature of the PLLA matrix due to a relatively low optical purity (98%) may be beneficial to the toughness as well. In the case of highly pure PLLA materials, e.g., L-content > 99.5%, it may crystallize and possess crystallinity after processing. Consequently, the resulting mechanical properties may be varied to a certain extent depending on the crystallinity and crystal morphology.

To provide a deeper insight in the mechanical behavior, stress−strain curves of the PLLA/PDLA blends were recorded, as shown in Figure 6. A digital image of the tested tensile bars is

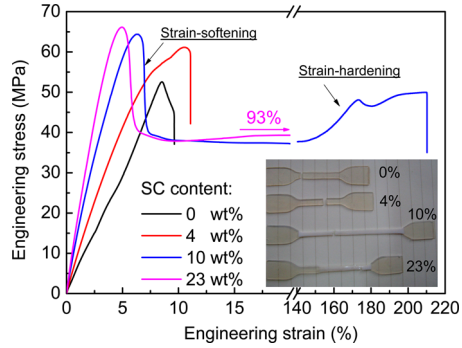

Figure 6. Stress−strain curves of the PLLA/PDLA blends as a function of SC-PLA concentration. A digital image of the tested tensile bars is presented as an inset showing neck-formation upon stretching and optical clarity of the samples.

presented as an inset. PLLA broke as soon as it passed the yielding point, showing a pronounced strain-softening without back-up of strain-hardening. The strain-softening stimulates strain localization, which results in triaxial stresses upon stretching. If the triaxial stresses could not be delocalized efficiently, failure of the matrix occurs, and thus brittleness of PLLA.[53] On the other hand, the PLLA/PDLA blend with 10 wt % of SC-PLA exhibits strain-softening followed by a stable neck-growth (inset of Figure 6) and strain-hardening. Strain-hardening is usually referred to stretching of the polymer network,[53] which is inconsistent with the aforementioned physical cross-link network in the PLLA/PDLA blends. In addition, the *E*-modulus of the blends was increased with SC-PLA content, as indicated by the enhanced slope of stress versus strain in the initial state.

Morphology and Toughening Mechanism. Crystallization plays a significant role in properties of semicrystalline polymer and polymer blends. For example, the impact toughness of PLA/EGMA blends was increased by of 10 times after annealing (crystallization) at 90 °C.[21] Afrifah et al. reported that the toughness of crystallized PLA/EAC blends was higher than that of amorphous PLA/EAC blends.[23] However, the present PLLA/PDLA blends contain rigid SC domains, which are different from rubbery EGMA and EAC copolymers, and the toughening mechanism is deduced from the local deformation of the drawn samples.

The neck region of the tensile bars, taking the PLLA/PDLA (90/10) blend as an example, was subjected to cryo-microtome analysis in the stretching direction and the morphology was

DOI: 10.1021/acssuschemeng.5b00208
ACS Sustainable Chem. Eng. 2015, 3, 1470−1478

observed by TEM, as shown in Figure 7. To compare the changes in morphology before and after elongation, the images

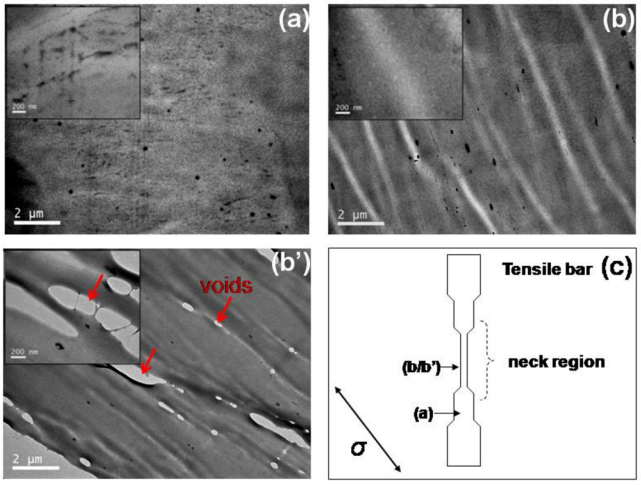

Figure 7. TEM images (scale bar = 2 μm) of stretched PLLA/PDLA (90/10) blend taken from different regions of a tested tensile bar, as schematically illustrated in panel c. Enlarged parts of the images are present as insets with a scale bar of 200 nm. The void formation in panel b′ is specified by arrows.

in both panels a and b/b′ were observed, as schematically shown in Figure 7c. Slight phase separation is distinguished in the PLLA/PDLA blends prior to deformation (Figure 7a) and a sheaf-like SC morphology is observed. After stretching, the randomly distributed sheaf-like SC-PLA grow into long fiber-like structures in the stretching direction (Figure 7b). The strongly increased phase contrast and the macroscopically stress-whitening phenomenon (inset of Figure 6) indicate larger (electron-) density differences between the stretched PLLA matrix and the SC domains. Upon drawing, stress can be transferred to the SC-PLA phase (concentrators) via interface. This leads to the extension and orientation of the SC-PLA chains without interfacial debonding due to a strong interfacial adhesion (inset of Figure 7b); however, the large deformation of the dispersed phase would absorb considerable stress energy, leading to a ductile behavior.[54] In addition, voiding is detected in some of the stretched regions, although it is not the dominating phenomenon (Figure 7b′). The concentrated stress results in voiding between lamellae or crystalline aggregations within the SC domains, which releases triaxial stress and prevents localization of strain in PLLA matrix, and hence a ductile behavior.[53,55] To obtain toughness by releasing such local stress, materials have to be designed as multiphase structures.[53] This explains the brittle behavior of neat PLLA and the ductile behavior of the asymmetric PLLA/PDLA where phase separation was induced by stereocomplexation. Inorganic fillers were used as well in the literature to toughen plastics, but no changes in geometry, whereas SC-PLA can be deformed bacause it is aggregations of regular crystals that connected via intermolecular force, which is different from conventional fillers.[30]

To summarize, the toughness of the asymmetric PLLA/PDLA blends resulted from the stereocomplexation-induced phase separation, which leads to (i) a physical cross-link network that can release stress in stretching (strain-hardening), (ii) easy deformation of the SC domains upon drawing that can absorb stress energy avoiding the crazing of PLLA matrix and (iii) voiding of the SC phase that delocalizes the stress/strain.

Transparency of the Asymmetric PLLA/PDLA Blends. Amorphous PLLA is usually transparent and becomes opaque after crystallization or incorporation of immiscible materials. The transmittance of visible light of the asymmetric PLLA/PDLA blends is presented in Figure 8. As expected, the PLLA

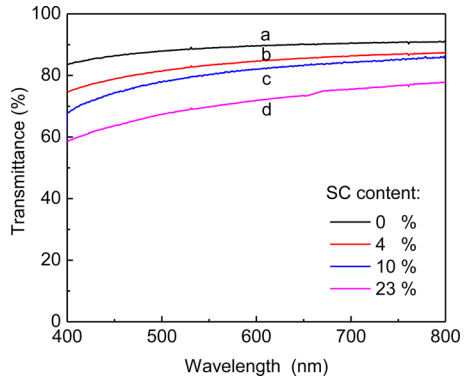

Figure 8. Light transmittance of asymmetric PLLA/PDLA sheets (1.0 mm in thickness) measured by a UV−visible light scattering device as a function of wavelength and SC-PLA concentration: (a) 0%, (b) 4%, (c) 10% and (d) 23%.

exhibits high transmittance (~90%) due to a low crystallinity (X_c = 2%, Figure 2). Interestingly, the PLLA/PDLA reserves high transmittance (~70%) even at a SC concentration of 10−23%. The reduction in transmittance after formation of SC-PLA is ascribed to the scattering effect of the SC domains. The average SC domain size is between 950 and 1200 nm, not much larger than the wavelength of visible light (390−780 nm), thus good transparency of the PLLA/PDLA blends remains after the stereocomplexation. The good transparency is no doubt an advantage for packaging application. Good optical clarity of the PLLA/PDLA blends is also demonstrated by the digital photos of the tensile bars, as shown in Figure 6.

Heat-Resistance of the Asymmetric PLLA/PDLA Blends. A simple annealing process (100 °C × 3 min) was performed on the PLLA and PLLA/PDLA (90/10) blend to study its effect on the heat resistance of these samples. In this work, the heat resistance was studied by using DMA. The changes in storage modulus (E') and loss modulus (E'') of these samples with temperature are shown in Figure 9. The PLLA and PLLA/PDLA blends (curves a and b, respectively) without annealing show steep reductions in E' at around 70 °C, which increased subsequently to around 100 °C due to the cold crystallization (T_{cc}, see the discussion of Figure 2). The E' of the PLLA was increased slightly after annealing at 100 °C for 3 min, e.g., from 4 to 34 MPa at 95 °C (curves a and a′ in Figure 9a). In contrast, the E' at 95 °C of the PLLA/PDLA blend was enhanced from 11 to 423 MPa after annealing and the high E' values were retained upon >130 °C (curves b to b′ in Figure 9a). These results indicate that (i) crystallization of the PLLA/PDLA blend was complete during the short annealing, thus no T_{cc} occurred upon heating and (ii) the SC-PLA enhanced the crystallization of PLLA remarkably during the annealing.[38] Peak temperatures of the G'' are referred to as T_g in this work and presented in Figure 9b. Obviously, the T_g of PLA was increased by 2−5 °C after completion of crystallization. In the literature, an increase in E' was obtained in PLLA/PDLA/PMMA system as well by annealing the samples at 110 °C for 20 min, which

DOI: 10.1021/acssuschemeng.5b00208
ACS Sustainable Chem. Eng. 2015, 3, 1470−1478

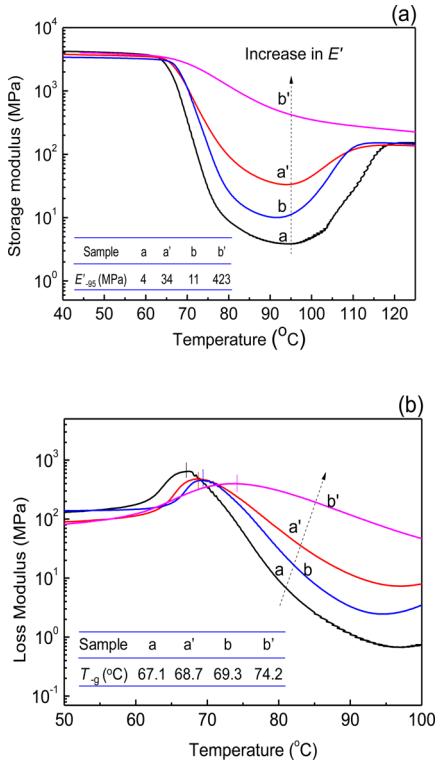

Figure 9. Dynamic mechanical properties of the PLLA and PLLA/PDLA (90/10) blend as a function of temperature: (a) storage modulus (E') and (b) loss modulus (E''). Curves a and a′ correspond to the PLLA before and after annealing at 100 °C for 3 min respectively, and curves b and b′ correspond to the PLLA/PDLA (90/10) blend before and after annealing at 100 °C for 3 min, respectively. The E' at 100 °C and the T_g referring to the peak temperature of E'' of the samples are inset into panels a and b, respectively.

was ascribed to massive crystallization of the PLA stereocomplex.[36] Therefore, high heat-resistance of the asymmetric PLLA/PDLA blends in this work can be achieved via a shorter annealing process at lower temperatures. It has to be remarked that the average light transmittance (wavelength from 400 to 800 nm) of the PLLA and the PLLA/PDLA (90/10) blend was decreased by 89% and 75%, respectively, after the annealing due to the scattering effect of enhanced crystals.

CONCLUSION

Asymmetric PLLA/PDLA blends were prepared via melt compounding at 200 °C. The stereocomplexation behavior and the resulting microstructures of the blends were studied by using WAXD, DSC, rheometer and Molau experiments. The SC-PLA concentration varied from 0 to 23% with increasing the PDLA content up to 20 wt % while very little PLA homocrystals (HC-PLA) was obtained in the PLLA/PDLA blends. The SC-PLA domains resulted in a physical cross-link network that wat confirmed by the frequency-independence of storage modulus/tan δ in rheological measurement and the gel in chloroform. Further analysis revealed that the SC-PLA domains were dominantly connected via entanglement of partially free chains when the SC-PLA concentration was lower than 10% (Structure I), whereas the adjacent SC-PLA domains were mainly bridged by molecules involved in both crystalline domains at SC-PLA concentrations higher than 23% (Structure II). The existence of rigid SC-PLA domains and network reinforced the PLLA, which is proven by an increase in melt viscosity, modulus and yield strength of the PLLA/PDLA blends. Surprisingly, the elongation at break of the PLLA/PDLA blends was enhanced by 20 times after the stereocomplexation, i.e., from 11% to approximately 200%, displaying a notable brittle-to-ductile transition. The improved toughness is ascribed to an overall contribution of the SC-PLA network, easy deformation and cavitation of SC-PLA domains in the presence of stress. The amorphous PLLA matrix result from a relatively low optical purity (98%) may also be beneficial to the toughness. In addition, the asymmetric PLLA/PDLA blends exhibit transmittance above 70% in the wavelength range of visible light, and by a simple annealing process good heat-resistance of the blends can be achieved as well. To summarize, full PLA materials with balanced and superior properties such as melt processability, high yield strength, toughness, transparency and heat-resistance can be obtained via stereocomplexation. Thus, this study goes beyond pure academic interest and may enable a larger application range of PLA materials.

AUTHOR INFORMATION

Corresponding Authors

*P. Ma. E-mail: p.ma@jiangnan.edu.cn. Tel.: +86 510 85917019.

*M. Chen. E-mail: mqchen@jiangnan.edu.cn. Tel.: +86 510 85917019.

Notes

The authors declare no competing financial interest.

ACKNOWLEDGMENTS

This work is supported by the National Natural Science Foundation of China (51303067) and the Natural Science Foundation of Jiangsu Province (BK20130147).

REFERENCES

(1) Gross, R. A.; Kalra, B. Biodegradable polymers for the environment. *Science* **2002**, *297*, 803−807.

(2) Schmack, G.; Tändler, B.; Vogel, R.; Beyreuther, R.; Jacobsen, S.; Fritz, H. G. Biodegradable fibers of poly(L-lactide) produced by high-speed melt spinning and spin drawing. *J. Appl. Polym. Sci.* **1999**, *73*, 2785−2797.

(3) Kim, J. K.; Park, D. J.; Lee, M. S.; Ihn, K. J. Synthesis and crystallization behavior of poly(L-lactide)-block-poly(ε-caprolactone) copolymer. *Polymer* **2001**, *42*, 7429−7441.

(4) Martin, O.; Avérous, L. Poly(lactic acid): Plasticization and properties of biodegradable multiphase systems. *Polymer* **2001**, *42*, 6209−6219.

(5) Rasal, R. M.; Janorkar, A. V.; Hirt, D. E. Poly(lactic acid) modifications. *Prog. Polym. Sci.* **2010**, *35*, 338−356.

(6) Hiljanen, V. M.; Karjalainen, T.; Seppälä, J. Biodegradable lactone copolymers. I. Characterization and mechanical behavior of ε-caprolactone and lactide copolymers. *J. Appl. Polym. Sci.* **1996**, *59*, 1281−1288.

(7) Grijpma, D. W.; Van Hofslot, R. D. A.; Super, H.; Nijenhuis, A. J.; Pennings, A. J. Rubber toughening of poly(lactide) by blending and block copolymerization. *Polym. Eng. Sci.* **1994**, *32*, 1674−1684.

(8) Gramlich, W. M.; Robertson, M. L.; Hillmyer, M. A. Reactive compatibilization of poly(L-lactide) and conjugated soybean oil. *Macromolecules* **2010**, *43*, 2313−2321.

(9) Ljungberg, N.; Wesslen, B. Preparation and properties of plasticized poly(lactic acid) films. *Biomacromolecules* **2005**, *6*, 1789−1796.

(10) Ma, P.; Spoelstra, A. B.; Schmit, P.; Lemstra, P. J. Toughening of poly(lactic acid) by poly(β-hydroxybutyrate-co-β-hydroxyvalerate)

DOI: 10.1021/acssuschemeng.5b00208
ACS Sustainable Chem. Eng. 2015, 3, 1470−1478

with high β-hydroxyvalerate content. *Eur. Polym. J.* **2013**, *49*, 1523−1531.
(11) Byrne, N.; Hameed, N.; Werzer, O.; Guo, Q. The preparation of novel nanofilled polymer composites using poly(L-lactic acid) and protein fibers. *Eur. Polym. J.* **2011**, *47*, 1279−1283.
(12) Broz, M. E.; VanderHart, D. L.; Washburn, N. R. Structure and mechanical properties of poly(D,L-lactic acid)/poly(ε-caprolactone) blends. *Biomaterials* **2003**, *24*, 4181−4190.
(13) Semba, T.; Kitagawa, K.; Ishiaku, U. S.; Hamada, H. The effect of crosslinking on the mechanical properties of polylactic acid/polycaprolactone blends. *J. Appl. Polym. Sci.* **2006**, *101*, 1816−1825.
(14) Wang, R.; Wang, S.; Zhang, Y.; Wan, C.; Ma, P. Toughening modification of PLLA/PBS blends via in situ compatibilization. *Polym. Eng. Sci.* **2009**, *49*, 26−33.
(15) Yokohara, T.; Yamaguchi, M. Structure and properties for biomass-based polyester blends of PLA and PBS. *Eur. Polym. J.* **2008**, *44*, 677−685.
(16) Ma, P.; Cai, X.; Zhang, Y.; Wang, S.; Dong, W.; Chen, M.; Lemstra, P. J. In-situ compatibilization of poly(lactic acid) and poly(butylenes adipate-co-terephthalate) blends by using dicumyl peroxide as a free-radical initiator. *Polym. Degrad. Stab.* **2014**, *102*, 145−151.
(17) Ojijo, V.; Sinha, R. S.; Sadiku, R. Toughening of biodegradable polylactide/poly(butylene succinateco-adipate) blends via in situ reactive compatibilization. *ACS Appl. Mater. Interfaces* **2013**, *5*, 4266−4276.
(18) Sun, Y.; He, C. Biodegradable "core−shell" rubber nanoparticles and their toughening of poly(lactides). *Macromolecules* **2013**, *46*, 9625−9633.
(19) Li, Y.; Shimizu, H. Toughening of polylactide by melt blending with a biodegradable poly(ether)urethane elastomer. *Macromol. Biosci.* **2007**, *7*, 921−928.
(20) Ma, P.; Hristova-Bogaerds, D. G.; Goossens, J. G. P.; Spoelstra, A. B.; Zhang, Y.; Lemstra, P. J. Toughening of poly(lactic acid) by ethylene-vinyl acetate copolymer with different vinyl acetate contents. *Eur. Polym. J.* **2012**, *48*, 146−154.
(21) Oyama, H. T. Super-tough poly(lactic acid) materials: Reactive blending with ethylene copolymer. *Polymer* **2009**, *50*, 747−751.
(22) Lebarbé, T.; Grau, E.; Gadenne, B.; Alfos, C.; Cramail, H. Synthesis of fatty acid-based polyesters and their blends with poly(L-lactide) as a way to tailor PLLA toughness. *ACS Sustainable Chem. Eng.* **2014**, *3*, 283−292.
(23) Afrifah, K. A.; Matuana, L. M. Impact modification of polylactide with a biodegradable ethylene/acrylate copolymer. *Macromol. Mater. Eng.* **2010**, *295*, 802−811.
(24) Ho, C. H.; Wang, C. H.; Lin, C. I.; Lee, Y. D. Synthesis and characterization of TPO-PLA copolymer and its behavior as compatibilizer for PLA/TPO blends. *Polymer* **2008**, *49*, 3902−3910.
(25) Chen, Y.; Yuan, D.; Xu, C. Dynamically vulcanized biobased polylactide/natural rubber blend material with continuous cross-linked rubber phase. *ACS Appl. Mater. Interfaces* **2014**, *6*, 3811−3816.
(26) Jandas, P. J.; Mohanty, S.; Nayak, S. K. Morphology and thermal properties of renewable resource-based polymer blend nanocomposites influenced by a reactive compatibilizer. *ACS Sustainable Chem. Eng.* **2013**, *2* (3), 377−386.
(27) Zhang, C.; Man, C.; Pan, Y.; Wang, W.; Jiang, L.; Dan, Y. Toughening of polylactide with natural rubber grafted with poly(butyl acrylate). *Polym. Int.* **2011**, *60*, 1548−1555.
(28) Li, H.; Huneault, M. A. Effect of nucleation and plasticization on the crystallization of poly(lactic acid). *Polymer* **2007**, *48*, 6855−6866.
(29) Ogata, N.; Jimenez, G.; Kawai, H.; Ogihara, T. Structure and thermal/mechanical properties of poly(L-lactide)-clay blend. *J. Polym. Sci., Part B: Polym. Phys.* **1997**, *35*, 389−396.
(30) Ray, S. S.; Yamada, K.; Okamoto, M.; Fujimoto, Y.; Ogami, A.; Ueda, K. New polylactide/layered silicate nanocomposites. 5. Designing of materials with desired properties. *Polymer* **2003**, *44*, 6633−6646.
(31) Ikada, Y.; Jamshidi, K.; Tsuji, H.; et al. Stereocomplex formation between enantiomeric poly(lactides). *Macromolecules* **1987**, *20*, 904−906.
(32) Tsuji, H.; Hyon, S. H.; Ikada, Y. Stereocomplex formation between enantiomeric poly(lactic acid)s. 3. Calorimetric studies on blend films cast from dilute solution. *Macromolecules* **1991**, *24*, 5651−5656.
(33) Tsuji, H.; Hyon, S. H.; Ikada, Y. Stereocomplex formation between enantiomeric poly(lactic acid)s. 4. Differential scanning calorimetric studies on precipitates from mixed solutions of poly(D-lactic acid) and poly(L-lactic acid). *Macromolecules* **1991**, *24*, 5657−5662.
(34) Tsuji, H.; Ikada, Y. Stereocomplex formation between enantiomeric poly(lactic acid)s. 6. Binary blends from copolymers. *Macromolecules* **1992**, *25*, 5719−5723.
(35) Tsuji, H.; Ikada, Y. Stereocomplex formation between enantiomeric poly(lactic acid)s. 9. Stereocomplexation from the melt. *Macromolecules* **1993**, *26*, 6918−6926.
(36) Samuel, C.; Cayuela, J.; Barakat, I.; Müller, A. J.; Raquez, J. M.; Dubois, P. Stereocomplexation of polylactide enhanced by poly(methyl methacrylate): Improved processability and thermomechanical properties of stereocomplexable polylactide-based materials. *ACS Appl. Mater. Interfaces* **2013**, *5*, 11797−11807.
(37) Bao, R. Y.; Yang, W.; Wei, X. F.; Xie, B. H.; Yang, M. B. Enhanced formation of stereocomplex crystallites of high molecular weight poly(L-lactide)/poly(D-lactide) blends from melt by using poly(ethylene glycol). *ACS Sustainable Chem. Eng.* **2014**, *2*, 2301−2309.
(38) Wei, X. F.; Bao, R. Y.; Cao, Z. Q.; Yang, W.; Xie, B. H.; Yang, M. B. Stereocomplexation and morphology of polylactides. *Macromolecules* **2014**, *47*, 1439−1448.
(39) Rahman, N.; Kawai, T.; Matsuba, G.; Nishida, K.; Kanaya, T.; Watanabe, H.; Honma, N. Effect of polylactide stereocomplex on the crystallization behavior of poly(L-lactic acid). *Macromolecules* **2009**, *42*, 4739−4745.
(40) Brochu, S.; Prud'Homme, R. E.; Barakat, I.; Jerome, R. Stereocomplex crystallite network in asymmetric PLLA/PDLA blends: Formation, structure, and confining effect on the crystallization rate of homocrystallites. *Macromolecules* **1995**, *28*, 5230−5239.
(41) Tsuji, H.; Ikada, Y. Stereocomplex formation between enantiomeric poly(lactic acid)s. XI. Mechanical properties and morphology of solution-cast films. *Polymer* **1999**, *40*, 6699−6708.
(42) Tsuji, H. In vitro hydrolysis of blends from enantiomeric poly(lactide)s. Part 4: Well-homo-crystallized blend and nonblended films. *Biomaterials* **2003**, *24*, 537−547.
(43) Cartier, L.; Okihara, T.; Lotz, B. Triangular polymer single crystals: Stereocomplexes, twins, and frustrated structures. *Macromolecules* **1997**, *30*, 6313−6322.
(44) Ma, P.; Wang, R.; Wang, S.; Zhang, Y.; Zhang, Y. X.; Hristova, D. Effects of fumed silica on the crystallization behavior and thermal properties of poly(hydroxybutyrate-co-hydroxyvalerate). *J. Appl. Polym. Sci.* **2008**, *108*, 1770−1777.
(45) Xu, Z.; Zhang, Y.; Wang, Z.; Sun, N.; Li, H. Enhancement of electrical conductivity by changing phase morphology for composites consisting of polylactide and poly(ε-caprolactone) filled with acid-oxidized multiwalled carbon nanotubes. *ACS Appl. Mater. Interfaces* **2011**, *3*, 4858−4864.
(46) Xu, Z.; Niu, Y.; Yang, L.; Xie, W.; Li, H.; Gan, Z.; Wang, Z. Morphology, rheology and crystallization behavior of polylactide composites prepared through addition of five-armed star polylactide grafted multiwalled carbon nanotubes. *Polymer* **2010**, *51*, 730−737.
(47) Coppola, S.; Acierno, S.; Grizzuti, N.; Vlassopoulos, D. Viscoelastic behavior of semicrystalline thermoplastic polymers during the early stages of crystallization. *Macromolecules* **2006**, *39* (4), 1507−1514.
(48) Horst, R. H.; Winter, H. H. Stable critical gels of a copolymer of ethene and 1-butene achieved by partial melting and recrystallization. *Macromolecules* **2000**, *33*, 7538−7543.

DOI: 10.1021/acssuschemeng.5b00208
ACS Sustainable Chem. Eng. 2015, 3, 1470−1478

(49) Sarasua, J. R.; Arraiza, A. L.; Balerdi, P.; Maiza, I. Crystallinity and mechanical properties of optically pure polylactides and their blends. *Polym. Eng. Sci.* **2005**, *45*, 745−753.
(50) Othman, N.; Xu, C.; Mehrkhodavandi, P.; Hatzikiriakos, S. G. Thermorheological and mechanical behavior of polylactide and its enantiomeric diblock copolymers and blends. *Polymer* **2012**, *53*, 2443−2452.
(51) Tsuji, H.; Takai, H.; Saha, S. K. Isothermal and non-isothermal crystallization behavior of poly(L-lactic acid): Effects of stereocomplex as nucleating agent. *Polymer* **2006**, *47*, 3826−3837.
(52) Liu, Y.; Shao, J.; Sun, J.; Zhang, X.; Xin, J.; Miao, Q.; Wang, J. Improved mechanical and thermal properties of PLLA by solvent blending with PDLA-b-PEG-b-PDLA. *Polym. Degrad. Stab.* **2014**, *101*, 10−17.
(53) Meijer, H. E. H.; Govaert, L. E. Mechanical performance of polymer systems: The relation between structure and properties. *Prog. Polym. Sci.* **2005**, *30*, 915−938.
(54) Ma, P.; Hristova-Bogaerds, D. G.; Lemstra, P. J.; Zhang, Y.; Wang, S. Toughening of PHBV/PBS and PHB/PBS blends via in situ compatibilization using dicumyl peroxide as a free-radical grafting initiator. *Macromol. Mater. Eng.* **2012**, *297*, 402−410.
(55) L'Abee, R. M. A.; Van Duin, M.; Spoelstra, A. B.; Goossens, J. G. P. The rubber particle size to control the properties-processing balance of thermoplastic/cross-linked elastomer blends. *Soft Matter* **2010**, *6*, 1758−1768.

DOI: 10.1021/acssuschemeng.5b00208
ACS Sustainable Chem. Eng. 2015, 3, 1470−1478